# PSAT1 regulated by STAT4 enhances the proliferation, invasion and migration of ovarian cancer cells via the PI3K/AKT pathway

XIAO LI[1], SHUANG WANG[2], XIN NIE[1], YUEXIN HU[1], OUXUAN LIU[1], YUXUAN WANG[1] and BEI LIN[1]

[1]Department of Gynecology and Obstetrics, Shengjing Hospital of China Medical University, Shenyang, Liaoning 110004, P.R. China; [2]Department of Obstetrics and Gynaecology, Tianjin Central Hospital of Gynecology Obstetrics, Tianjin 300277, P.R. China

Received October 8, 2024; Accepted December 20, 2024

DOI: 10.3892/ijmm.2025.5529

**Abstract.** Epithelial ovarian cancer, the most prevalent form of ovarian cancer, is a health concern worldwide. Phosphoserine aminotransferase 1 (PSAT1), as the rate-limiting enzyme in serine synthesis, is key in the conversion of 3-phosphoglycerate to serine. The present study explored the role of PSAT1 expression in epithelial ovarian tumors. Gene Expression Profiling Interactive Analysis was used for gene expression and survival analyses. The effects of PSAT1 overexpression and knockdown on invasion, migration, proliferation and cell cycle progression of ovarian cancer cell lines were investigated both *in vitro* and *in vivo*. Western blotting was conducted to assess alterations in PI3K/AKT signalling pathway proteins. Database and tissue sample data confirmed that PSAT1 was significantly upregulated in ovarian cancer. Preliminary functional investigations indicated that PSAT1 was involved in modulation of invasion and migration, demonstrating the capacity of PSAT1 to enhance expression of the PI3K/AKT signalling pathway. These findings suggested that PSAT1 served a critical role in the onset and progression of ovarian cancer, thereby offering a theoretical basis for early detection and therapeutic strategies.

## Introduction

Among malignant tumors within the female reproductive system, ovarian cancer is recognized as the leading cause of mortality, thereby representing a public health concern. Among the various types of ovarian cancer, epithelial ovarian cancer accounts for 90% of all diagnosed cases (1). The majority of patients with epithelial ovarian cancer are diagnosed at advanced stages III or IV, where the corresponding 5-year survival rates are 42 and 26%, respectively (2). Despite advancements in surgical interventions and the routine utilization of chemotherapy and targeted therapeutics, the therapeutic efficacy of these modalities remains limited. Consequently, there is need to identify specific tumor markers and effective drug targets for accurate diagnosis, treatment and monitoring of ovarian cancer.

Abnormal cell proliferation is a hallmark of malignant tumors, and a notable association has been identified between control of cell cycle progression and the initiation of tumorigenesis (3). The PI3K/AKT pathway constitutes a key intracellular signaling cascade that regulates various physiological processes, including cell proliferation, survival, metabolism and migration (4,5). This pathway is ubiquitously expressed across diverse cell types and serves a cancer-promoting role in cancer and immune cells. The serine biosynthetic pathway is key in cancer metabolism. This pathway is governed by three key regulatory enzymes: Phosphoglycerate dehydrogenase (PHGDH), phosphoserine phosphatase and phosphoserine aminotransferase 1 (PSAT1). PSAT1 is the key enzyme in the serine synthesis pathway and catalyzes conversion of 3-phosphohydroxypyruvate to 3-phosphoserine, which is dephosphorylated subsequently to form L-serine participating in one-carbon metabolism and nucleic acid biosynthesis (6,7). Hence, PSAT1 activity is associated with onset and progression of tumorigenesis.

Our previous investigation confirmed that overexpression of PSAT1 is associated with poor prognosis of short overall survival time in ovarian cancer (8). Previous reports have revealed increased expression of PSAT1 in various types of malignancies, including colon cancer, esophageal squamous cell carcinoma and non-small cell lung cancer (9-12). However, the functional role of PSAT1 in ovarian carcinogenesis and the underlying molecular mechanisms remain to be fully delineated. The present study aimed to assess the impact of PSAT1 on development of ovarian tumors.

## Materials and methods

*Cell culture*. CAOV3, OVCAR3 and ES2 cell lines were purchased from Procell Life Science & Technology Co., Ltd. The A2780 cell line was purchased from Shanghai Biowing Applied Biotechnology Co., Ltd. The CAOV3, OVCAR3, A2780, and ES2 ovarian cancer cell lines were cultured in RPMI-1640 medium supplemented with 10% fetal bovine

*Correspondence to:* Professor Bei Lin, Department of Gynecology and Obstetrics, Shengjing Hospital of China Medical University, 36 Sanhao Street, Heping, Shenyang, Liaoning 110004, P.R. China
E-mail: blin@cmu.edu.cn

*Key words:* PSAT1, proliferation, invasion, metastasis, ovarian cancer

serum (both Biological Industries) at 37˚C and a 5% carbon dioxide.

*Establishment of stable PSAT1-overexpressing and transient PSAT1-knockdown cell lines*. A2780 and ES2 cell lines were transfected using *PSAT1*-CMV-MCS-IRES-EGFP-SV40-Neo mycin-mediated transfection (Shanghai Genechem Co., Ltd.). The cells were inoculated into 24-well cell culture plates at a density of 2,500 cells/well. RPMI-1640 culture medium, without serum, containing lentivirus was added to the cells for 12-18 h at 37˚C. The transfection concentration was 1 $\mu$g/$\mu$l (MOI=20). Transfection was performed using Lipofectamine 3000 (Invitrogen; Thermo Fisher Scientific, Inc.) according to the manufacturer's instructions. After 12 h, complete medium containing serum was added at 37˚C. ES2-PSAT1-high expression (H), ES2-PSAT1-H-Mock, A2780-PSAT1-H and A2780-PSAT1-H-Mock, were constructed. Subsequent experiments were performed after 24 h.

Efficiency of three small interfering (si)RNAs were detected by western blot. PSAT1-siRNA-3 was selected for subsequent experiments. PSAT1-siRNA and PSAT1-MOCK-siRNA sequences are shown in Table SI. PSAT1-siRNAs were transfected into CAOV3 and OVCAR3 cells. The working solutions for siRNA transfection were prepared according to the manufacturer's instructions (Shanghai GenePharma Co., Ltd.). The cells were seeded in 6-well plates with serum-free RPMI-1640 medium. The PSAT1 lentiviral was transfected at 37˚C for 48 h. Transfection was performed via Lipofectamine 3000 (Invitrogen; Thermo Fisher Scientific, Inc.) according to the manufacturer's instructions. The cells were collected 48 h after transfection and the effect of *PSAT1-siRNA* transfection was determined by western blotting. Within 48 h of transfection, cells were used for functional experiments and flow cytometric analysis. STAT4-siRNA was transfected into CAOV3 and OVCAR3 cells to establish CAOV3-STAT4-L and OVCAR3-STAT4-L, CAOV3-STAT4-Mock and OVCAR3-STAT4-Mock, CAOV3 and OVCAR3.

*Western blotting*. Following total protein extraction from CAOV3, OVCAR3, A2780 and ES2 cells, the cell pellet was lysed with precooled RIPA buffer (Beyotime Institute of Biotechnology) on ice for 30 min and centrifuged at 4˚C and 13.4 x g for 20 min. The supernatant was evaluated via BCA method to determine the total protein concentration in the lysate and 5X loading buffer was added for denaturation at 100˚C for 5 min. The samples were separated via 10% SDS-PAGE with 10 $\mu$g protein/lane, concentrated at 80 V and separated at 120 V, followed by electrotransfer at 4˚C and 100 V for 45-90 min to a PVDF membrane. Then, 5% skimmed milk or 5% bovine serum albumin (Biological Industries) was used for blocking at room temperature for 12 h. Cells were incubated with primary antibodies against PSAT1 (1:500; Abcam, ab308512), PI3K (1:1,000; Cell Signaling Technology, Inc.; cat. no. 4292S), phosphorylated (p-)PI3K (1:1,000; Cell Signaling Technology, 4228S), AKT (1:1,000; Cell Signaling Technology, 4691S), p-AKT (1:1,000; Cell Signaling Technology, Inc.; cat. no. 4691S) and GAPDH (1:4,000; Beijing Zhongshan Jinqiao Biotechnology, TA-08 Co., Ltd.) overnight at 4˚C. Samples were rinsed three times with 1X TBST for 10 min. Membranes were incubated with HRP-labelled goat anti-rabbit or goat anti-mouse (both 1:3,000; both Beijing Zhongshan Jinqiao Biotechnology Co., Ltd.) secondary antibodies for 1 h at 37˚C and then washed again. Finally, western chemiluminescent HRP substrate (Thermo Fisher Scientific, Inc.) was added dropwise onto the membrane, and luminescent signals were detected via a luminometer. Image Lab Software (Version 6.1; Bio-Rad was used for densitometry.

*Cell proliferation experiment*. A total of 2,000 ES-2 cells/well were seeded in 96-well culture plates and incubated at 37˚C in a 5% $CO_2$ incubator. After cells adhered to the wall, 20 $\mu$l sterile MTT (Beijing Solarbio Science & Technology Co., Ltd.) working solution was added to each well, mixed and incubated at 37˚C for 4 h. Subsequently, the medium was aspirated and 150 $\mu$l DMSO was added to each well. After shaking for 5 min, the absorbance at 490 nm of each well was measured via a microplate reader.

*Cell cycle analysis*. The ES-2 cells in the logarithmic growth phase were collected, washed with PBS and fixed with 70% ethanol overnight at 4˚C. A total of 500 $\mu$l PI/RNase A (Nanjing KeyGen Biotech Co., Ltd.) staining solution was added to the cell suspension according to the manufacturer's instructions and cells were incubated in the dark for 20 min at room temperature. The cells were analysed via flow cytometry of BD FACSAria and FlowJo (Version 10.7.2; both BD Biosciences).

*Invasion assay*. Transwell insert with pore size of 8 $\mu$m was placed in the culture plate. Matrigel (1:7.5; BD Biosciences) pre-coating was performed at 37˚C for 6 h and a serum-free $4x10^4$ ES-2 cell suspension were added to the upper chamber of RPMI-1640 medium and the lower chamber contained RPMI-1640 medium supplemented with 10% fetal bovine serum medium. After 48-72 h culture, cells were collected, fixed with 4% paraformaldehyde for 15 min at 37˚C and stained with crystal violet for 30 min at 37˚C. The number of cells in five randomly selected fields of view was counted and the mean of three repeated experiments was calculated. Light microscope was used to observe invasive cells.

*Migration experiment*. ES-2 cells were inoculated in 6-well plates and maintained in a 5% $CO_2$ incubator at 37˚C. After achieving 90% confluence, the cell layer was scratched with a 100-$\mu$l pipette suction head. The cells were cultured in serum-free medium for 24 h at 37˚C and washed with PBS. Images were obtained to monitor wound healing using a light microscope was used with magnification of 200. Quantification analysis was performed using ImageJ software.

*In vivo xenograft model of ovarian cancer*. The temperature of nude mice was about 20-26˚C and the relative humidity should be maintained at 40-60%. The experimental environment should maintain a 12 h light/dark cycle. Nude mice were provided with adequate food and water to ensure normal growth and metabolism. A total of 20 female nude mice (Huafukang Bioscience; age, 4-6 weeks; weight, 13-17 g) were randomly divided into two groups (n=10/group) and subcutaneously injected with ES2-PSAT1-Mock or ES2-PSAT1-H ovarian cancer cells (~$1x10^6$ cells in 100 $\mu$l PBS) into the

armpit of the left forelimb. Tumor progression and the overall health status of the mice were observed every 3 days and the diameter of the tumors and mouse weights were measured. The tumor volume was calculated as $V=(a \times b^2)/2$, where a represents the maximum diameter and b is the shortest diameter. At 7 days post-injection, newly formed tumors were detected. On day 21, mice began to show symptoms of poor health with the largest tumor diameter of 9.6 mm and maximum volume of 186.16 $mm^3$. The nude mice were completely sedated using isoflurane anesthesia (induction, 4%; maintenance, 1.5%). The animals were euthanized through exsanguination. Tumor samples were fixed at room temperature in 4% paraformaldehyde and embedded in paraffin for 24 h. Continuous 5-$\mu$m-thick sections were analysed via hematoxylin and eosin (HE) or immunohistochemical staining [including phosphorylated (p-)serine-threonine protein kinases (C-RAF) (Cell Signaling Technology, #9427, 1:100), p-AKT (Cell Signaling, #4060 1:200). Tissue sections were immersed in xylene, followed by dehydration in 100 and 80% ethanol for 5 min. The sections were rinsed in distilled water for 5 min, stained with hematoxylin for 5 min, and washed under running water for 10 min. Sections were counterstained with 0.5% eosin for 1-3 min and rinsed again in distilled water for 30 sec. For dehydration, sections were immersed in 80% ethanol for 30 sec, 95% ethanol for 1 min, and 100% ethanol for 3 min, followed by clearing in xylene for 3 min. Finally, the sections were mounted with neutral gum. The paraffin sections were deparaffinised with xylene and re-hydrated with gradient alcohol solutions, and the antigens were recovered by heating at 100˚C for 15 min. Subsequently, 3% hydrogen peroxide was added for 30 min at 37˚C, 10% goat serum blocking solution (Fuzhou Maixin Biotech Co., Ltd., KIT-9720) for 30 min at 37˚C, and anti-p-C-RAF antibody (Cell Signaling Technology, #9427, 1:100) or p-AKT (Cell Signaling Technology, #4060 1:200) was added overnight at 4˚C. The following day, the slices were incubated with biotin-labeled secondary antibody in complex with streptavidin-peroxidase (Fuzhou Maixin Biotech Co., Ltd., KIT-9720) for 30 min at 37˚C and stained using 3,3-diaminobenzidine and hematoxylin for 10 min at 37˚C.

Light microscope was used to observe. The brown granules observed in the nucleus and cytoplasm were scored; 0, 1, 2, and 3 corresponded to no coloration, light yellow, brownish-yellow, and tan, respectively. Additionally, scores of 0, 1, 2, 3, and 4 represented <5, 6-25%, 26-50%, 51-75%, and >75% of the visual field, respectively. The final score was calculated by multiplying the two aforementioned scores, with the following interpretations: 0-2 (-), 3-4 (+), 5-8 (++), and 9-12 (+++). Quantification analysis was performed using ImageJ software (V1.0; National Institutes of Health). The animal studies were approved by the Shengjing Hospital Affiliated to China Medical University Ethics Review Committee (approval no. 2021PS894K).

*Signalling pathway inhibition*. ES2-PSAT1-Mock or ES2-PSAT1-H ovarian cancer cells were cultured at 37˚C in the presence of PI3K inhibitor (PI3Ki; cat. no. GDC-0941, Selleck Chemicals) for 48 h. For inhibitor concentration selection, 5, 10, 15, 20, 25, 30, 35 and 40 $\mu$M were used during the preliminary experiment. When the inhibitor concentration reached 25 $\mu$M, further increases did not enhance the inhibitory effect. Therefore, 25 $\mu$M was used for subsequent experiments. Additionally, 0.1% DMSO served as the negative control.

*Gene expression profiling interactive analysis (GEPIA) dataset analysis*. The survival curves were generated using the GEPIA tool (gepia.cancer-pku.cn/), which integrated RNA-seq data and clinical survival information from The Cancer Genome Atlas) and GTEx databases. The dataset name was 'TCGA Pan-Cancer Clinical Data Resource', accessible via the GDC Data Portal (https://portal.gdc.cancer.gov/) under the project accession number 'phs000178.v11.p8' (13-15). Differential mRNA expression of PSAT1 between 426 cancerous samples and 88 normal ovarian tissue samples was evaluated.

*GeneMANIA analysis*. GeneMANIA (genemania.org) is a public database that provides a list of genes with similar functions for construction of interactive functional association networks and analysis of the relationships between genes and datasets. A gene interaction network for PSAT1 was constructed on the basis of physical interactions, predictions, colocalization, co-expression, signalling pathway information and predicted functions.

*Promo and JASPAR database analysis*. Promo (alggen.lsi.upc.es/cgi-bin/promo_v3/promo/promoinit.cgi?dirDB=TF_8.3) is a tool for identifying potential transcription factor binding sites in DNA sequences, which predicts transcription factor binding sites by constructing a matrix of specific binding site weights (16). JASPAR (https://jaspar.elixir.no/) is an open access database that stores manually curated transcription factor binding preferences as a position frequency matrix (17). Promo and JASPAR databases were used to predict that STAT4 functions as a transcriptional regulator of PSAT1 expression.

*Statistical analysis*. SPSS 22.0 (IBM Corp.) was used for the statistical analyses. All the data are presented as the mean ± standard deviation of three independent repeats. The data were analyzed using $\chi^2$ and Fisher's exact probability test. Statistical differences between two groups were determined using the unpaired t test, and one-way analysis of variance analysis followed by Scheffe's test was used for the comparison of >2 groups. Two-sided $P<0.05$ was considered to indicate a statistically significant difference.

## Results

*Expression of PSAT1 is higher in cancer tissue*. Through GEPIA, in-depth analysis was conducted to elucidate differential mRNA expression patterns of PSAT1 between ovarian cancer and normal samples. PSAT1 mRNA was significantly upregulated in ovarian cancer compared with normal tissue (Fig. 1A). Immunohistochemical analysis revealed PSAT1 expression in ES2, A2780, CAOV3 and OVCAR3 cell lines (Fig. 1B). Western blotting demonstrated higher PSAT1 protein expression in CAOV3 and OVCAR3 than in ES2 and A2780 cells, however this was not significant (Fig. 1C and D).

To establish a cell model with decreased PSAT1 expression, CAOV3 and OVCAR3 ovarian cancer cell lines, which exhibited relatively high PSAT1 expression were used. ES2 and A2780

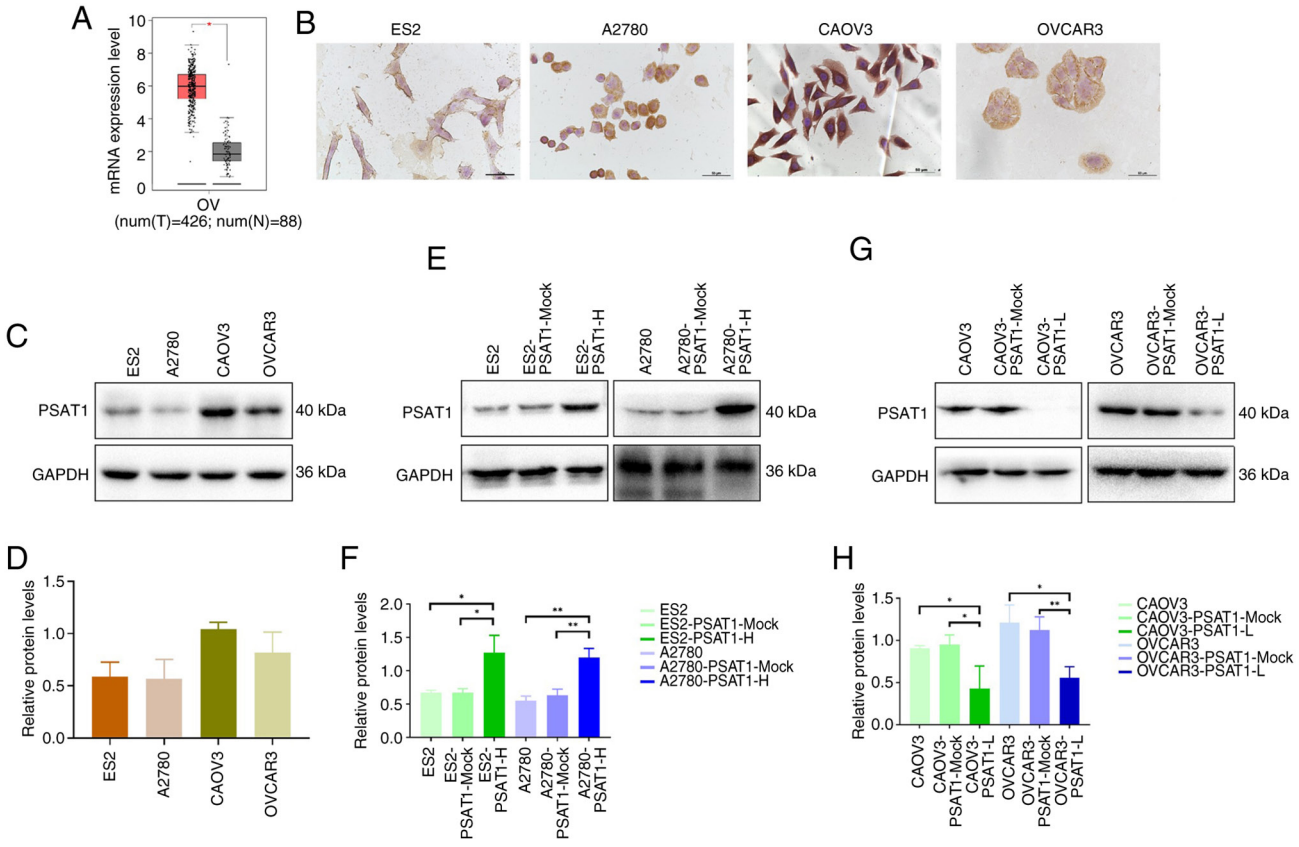


Figure 1. PSAT1 expression in ovarian cancer tissue and cells. (A) Differential mRNA expression of PSAT1 between ovarian cancer and normal ovarian tissues in the Gene Expression Profiling Interactive Analysis database. (B) Expression of PSAT1 in ES2, A2780, CAOV3 and OVCAR3 cell lines was detected by immunohistochemistry. (C) PSAT1 expression is higher in CAOV3 and OVCAR3 than in ES2 and A2780 cells. Magnification, x200. (D) Relative expression levels of PSAT1 in ES2, A2780, CAOV3, and OVCAR3 cell lines. (E) Construction of stable and high PSAT1 of ES2 and A2780 cell lines. (F) Quantitative analysis of relative expression levels of PSAT1 in ES2 and A2780 cell lines with PSAT1 overexpression. (G) Construction of PSAT1-L in CAOV3 and OVCAR3 cell lines. (H) Quantitative analysis of relative expression levels of PSAT1 in CAOV3 and OVCAR3 cell lines with PSAT1 knockdown. PSAT, phosphoserine aminotransferase; H, high; L, low; OV, OVCAR3; T, tumor; N, normal. $^{*}$P<0.05, $^{**}$P<0.01.

ovarian cancer cell lines, characterized by comparatively low PSAT1 expression, were used to generate a cell model with overexpressed PSAT1. Three sequences of siRNA have been screened by western blot to obtain the one with the best knockdown effect (Fig. S1). Western blot analysis revealed that the ES2-PSAT1-H and A2780-PSAT1-H cells presented significantly elevated PSAT1 expression compared with control cells (ES2-PSAT1-Mock, ES2, A2780-PSAT1-Mock and A2780). By contrast, the PSAT1 protein levels were significantly lower in CAOV3-PSAT1-L and OVCAR3-PSAT1-L cells than in the corresponding control cells (CAOV3-PSAT1-Mock, CAOV3, OVCAR3-PSAT1-Mock and OVCAR3; Fig. 1E-H).

*PSAT1 promotes proliferation, invasion and migration of ovarian cancer cells*. MTT assay was used to determine proliferation of ovarian cancer cells following the overexpression or knockdown of PSAT1. The impact of PSAT1 upregulation and suppression on the cell cycle was assessed via flow cytometry analysis. ES2-PSAT1-H and A2780-PSAT1-H cell lines exhibited significantly greater proliferation and a greater proportion of cells in the G2/M phase than their respective control (ES2-PSAT1-Mock, ES2, A2780-PSAT1-Mock and A2780). Conversely, CAOV3-PSAT1-L and OVCAR3-PSAT1-L lines demonstrated significantly decreased proliferation and proportion of cells within G2/M phase relative to the control groups (CAOV3-PSAT1-Mock, CAOV3, OVCAR3-PSAT1-Mock and OVCAR3; Fig. 2). These findings underscored the capacity of PSAT1 to promote proliferation of ovarian cancer cells.

Transwell and scratch assays were conducted to investigate the impact of PSAT1 on the invasive and migratory capacity of ovarian cancer cells. The invasive and migratory potential of the ES2-PSAT1-H and A2780-PSAT1-H cells was significantly greater than that of the ES2-PSAT1-Mock, ES2, A2780-PSAT1-Mock and A2780 control cells. By contrast, CAOV3-PSAT1-L and OVCAR3-PSAT1-L cells exhibited significantly decreased invasion and migration compared with CAOV3-PSAT1-Mock, CAOV3, OVCAR3-PSAT1-Mock and OVCAR3 (Fig. 3). These findings suggested that PSAT1 enhanced the invasive and migratory potential of ovarian cancer cells.

*PSAT1 promotes tumor formation in vivo*. To investigate the influence of PSAT1 on the tumorigenesis of ovarian cancer cells, ES2-PSAT1-H cells and ES2-PSAT1-Mock cells were subcutaneously implanted into athymic nude mice (Fig. 4A). After 21 days, the mean tumor volume in the ES2-PSAT1-H cells was significantly greater than that in the control group. Additionally, the mean tumor weight in the PSAT1-overexpression cohort was ~3.32 times greater than that in the control cohort (Fig. 4B and C). The tumor xenografts from the nude mice were processed for histological analysis. The protein expression levels of p-C-RAF and p-AKT in the

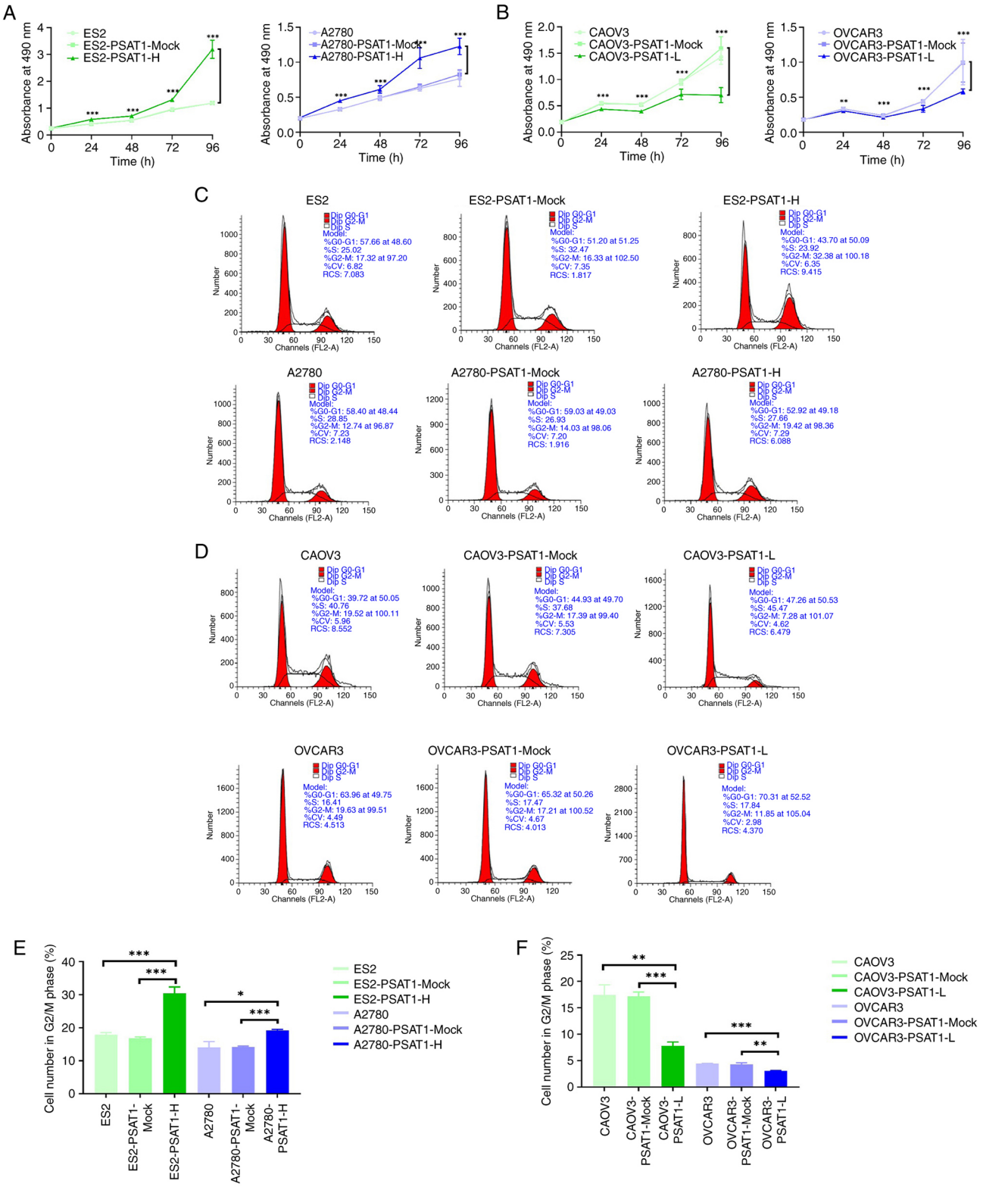


Figure 2. Effect of PSAT1 on proliferation of ovarian cancer cells. (A) PSAT1 overexpression promotes the proliferation of ES2 and A2780 ovarian cancer cells, as determined via the MTT assay. (B) PSAT1-L inhibits proliferation of ovarian cancer cells in MTT assay in CAOV3 and OVCAR3 cell lines. (C) Ovarian cells passed into S and G2/M phases after PSAT1 overexpression. (D) G0/G1 phase arrest of ovarian cancer cells following PSAT1 siRNA transfection. (E) Cell cycle distribution in ES2 and A2780 cell lines with PSAT1 overexpression. (F) Statistical analysis of cell cycle in CAOV3 and OVCAR3 cell lines with PSAT1 knockdown. PSAT, phosphoserine aminotransferase; si, small interfering; L, low; H, high. Asterisks indicate statistically significant differences compared to the control group. $^{*}$P<0.05, $^{**}$P<0.01; $^{***}$P<0.001 vs. control.

ES2-PSAT1-H group were notably elevated compared with those in the ES2-PSAT1-Mock group, indicating that PSAT1 can facilitate tumor cell proliferation *in vivo*.

*PSAT1 promotes proliferation, invasion and migration of ovarian cancer cells via the PI3K/AKT pathway*. GeneMANIA database was used to construct a gene-gene interaction network

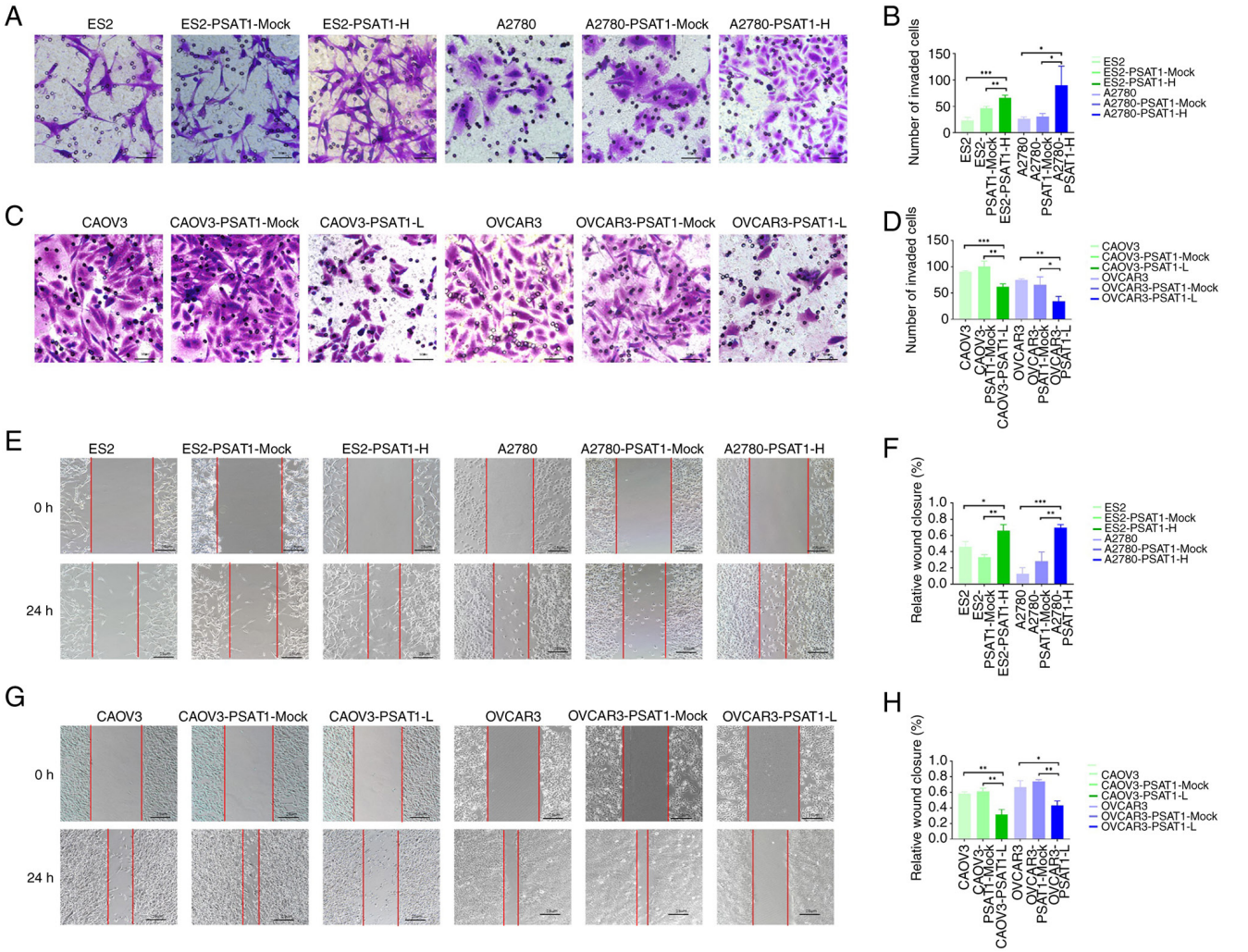


Figure 3. Effect of PSAT1 on invasion and migration of ovarian cancer cells. (A) Effects of PSAT1 overexpression on (B) invasion of ES2 and A2780 cells. (C) PSAT1-siRNA suppresses (D) invasion of OVCAR3 and CAOV3 cells. Scale bar, 100 $\mu$m. (E) Effects of PSAT1 overexpression on migration of ES2 and A2780 cells (x10). (F) Statistical analysis of cell migration ability in ES2 and A2780 cell lines with PSAT1 overexpression. (G) PSAT1-siRNA suppresses migration of OVCAR3 and CAOV3 cells. (H) Statistical analysis of migration ability in CAOV3 and OVCAR3 cell lines with PSAT1 knockdown. PSAT, phosphoserine aminotransferase; si, small interfering; L, low; H, high. $^{*}$P<0.05; $^{**}$P<0.01; $^{***}$P<0.001; vs. control.

for *PSAT1*. The five genes demonstrating the greatest association with *PSAT1* were programmed cell death 11, ubiquitin-like modifier activating enzyme 1, peptidylprolyl isomerase D, heparan sulfate proteoglycan 2 and *PHGDH* (Fig. 5A). Western blotting was used to determine the expression levels of p-PI3K, PI3K, p-AKT and AKT. Expression of p-PI3K and p-AKT was significantly lower in CAOV3-PSAT1-L than in the control groups CAOV3-PSAT1-Mock and CAOV3 (Fig. 5B and C). These findings confirmed that PSAT1 modulated the PI3K/AKT signalling pathway in ovarian cancer cells.

Promo and JASPAR databases were used to predict that STAT4 functions as a transcriptional regulator of PSAT1 expression. Western blot analysis confirmed that protein expression levels of PSAT1 in CAOV3-STAT4-L and OVCAR3-STAT4-L cell lines were significantly lower than those in the CAOV3-STAT4-Mock, CAOV3, OVCAR3-STAT4-Mock and OVCAR3 controls (Fig. 5D and E).

*PI3K pathway inhibition decreases proliferation, invasion and migration ability of PSAT1-overexpressing cells*. To explore the effect of PSAT1 on the PI3K pathway, PI3Ki GDC-0941 was used. Proliferation of ES2-PSAT1-H cells was greater than that of control cells. However, GDC-0941 significantly diminished the increase in proliferation induced by PSAT1 (Fig. 6A). Flow cytometry revealed that the ratio of G2/M phase cells in the ES2-PSAT1-H group was significantly increased compared with ES2-PSAT1-Mock, and GDC-0941 significantly decreased the proportion of G2/M phase cells (Fig. 6B and C). PSAT1 promoted ovarian cancer cell entry into G2/M phase and promoted cell proliferation via the PI3K signalling pathway. The PI3K inhibitor GDC-0941 attenuated this proliferation (Fig. 6B and C). Transwell assay revealed invasion ability of ES2-PSAT1-H cells was enhanced compared with ES2-PSAT1-Mock, and the addition of PI3Ki significantly reduced the invasion ability (Fig. 6D and E). The results of the scratch assay revealed that the migration ability of ES2-PSAT1-H cells was increased compared with ES2-PSAT1-Mock and the addition of PI3Ki significantly decreased the PSAT1 overexpression-induced increase in migration (Fig. 6F and G). Collectively, these results demonstrated that PSAT1 affected the proliferation, invasion

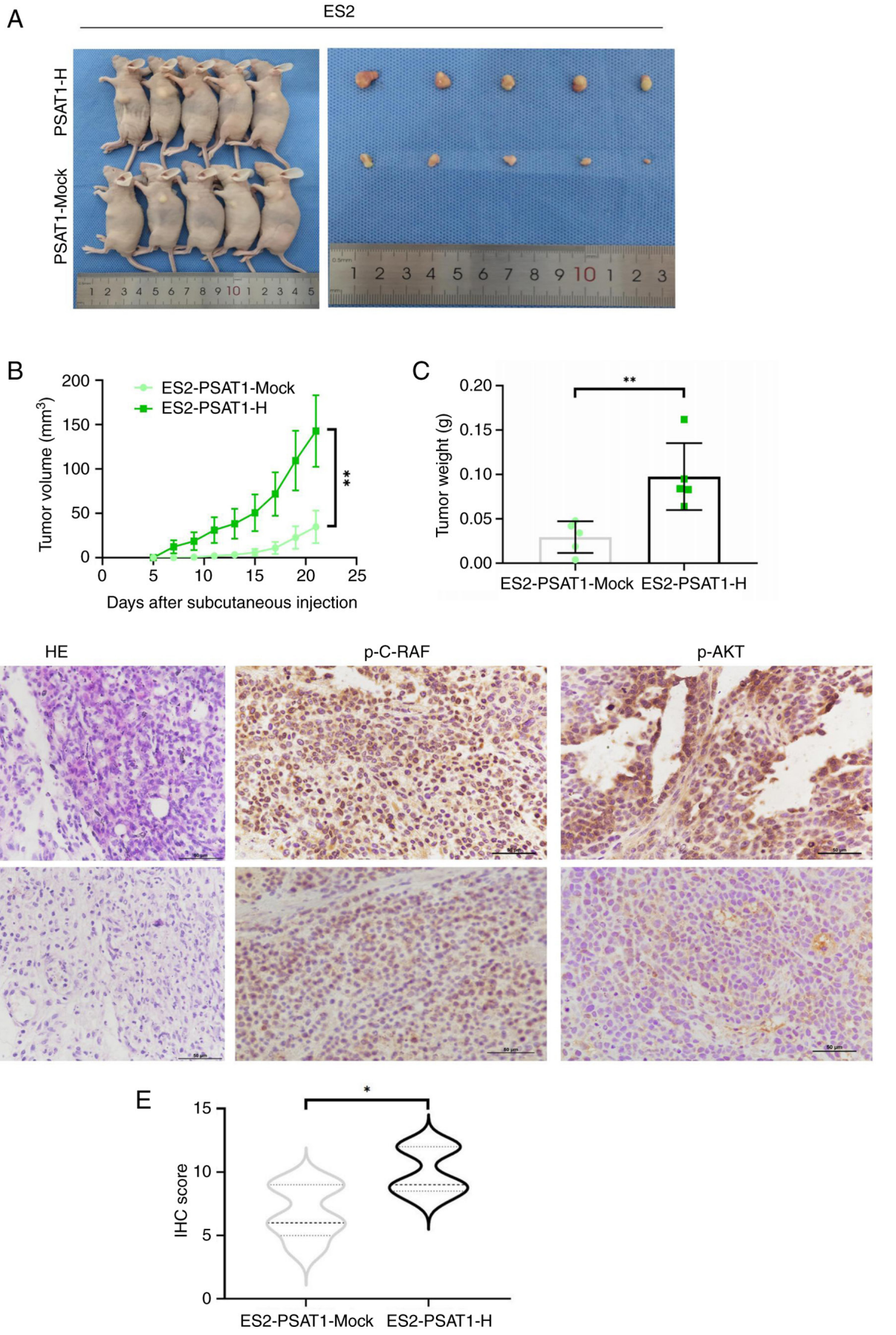


Figure 4. Effect of PSAT1 on tumor formation *in vivo*. (A) Subcutaneous xenografts of nude mice. (B) Changes in the volume and quality of tumors. (C) Tumor weights and volumes in subcutaneous xenografts of nude mice with PSAT1 overexpression. (D) HE and immunohistochemistry staining of p-C-RAF and p-AKT. (E) Statistical analysis of IHC scoring of p-C-RAF and p-AKT. PSAT, phosphoserine aminotransferase; IHC, immunohistochemistry; HE, hematoxylin and eosin; p-, phosphorylated; C-RAF, serine-threonine protein kinases); H, high. $^{*}$P<0.05, $^{**}$P<0.01.

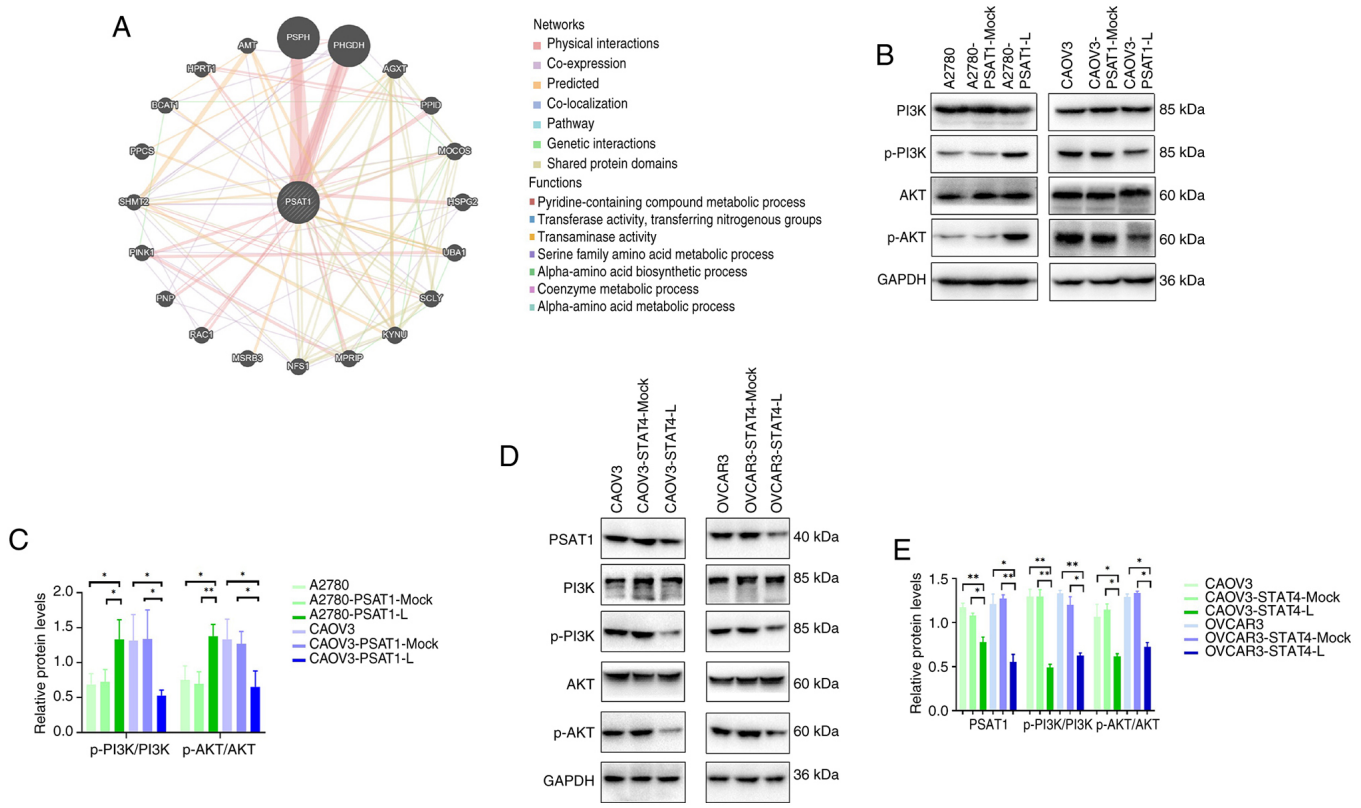


Figure 5. PSAT1 exerts cellular effects through the PI3K/AKT signalling pathway. (A) Construction of the PSAT1 gene interaction network using GeneMANIA. (B) Expression of p-PI3K, PI3K, p-AKT and AKT in ovarian cancer cells. (C) Quantitative analysis of relative expression levels of p-PI3K, PI3K, p-AKT and AKT in ovarian cancer cells. (D) PSAT1, p-PI3K/PI3K, p-AKT/AKT protein expression levels in CAOV3-STAT4-L and OVCAR3-STAT4-L cells were lower than those in CAOV3-STAT4-Mock, CAOV3, OVCAR3-STAT4-Mock and OVCAR3 cells. (E) Quantitative analysis of relative expression of PSAT1, p-PI3K/PI3K, p-AKT/AKT in CAOV3 and OVCAR3 cell lines with STAT4 knockdown. PSAT, phosphoserine aminotransferase; p-, phosphorylated; L, low; H, high. $^{*}$P<0.05; $^{**}$P<0.01; vs. control.

and migration ability of ovarian cancer cells via the PI3K signalling pathway.

## Discussion

Serine is a critical component for cellular proliferation, folate metabolism, phospholipid metabolism and the formation of d-serine and glycine, which serve as neuromodulators (18). Restriction of serine availability notably affects development and functionality of the central nervous system. Individuals with serine deficiency may exhibit serious neurological or psychiatric disorder, including epilepsy, severe psychomotor retardation and congenital microcephaly (19). PSAT1, a member of the class V pyridoxal phosphate-dependent aminotransferase family, serves a key role in the serine biosynthetic pathway (20). Mutations within PSAT1, encoding the second enzyme in the serine biosynthetic cascade, are associated with a form of serine deficiency known as PSAT1 deficiency (21). However, clinical diagnosis of PSAT1 deficiency solely on the basis of the measurement of serine levels in cerebrospinal fluid is challenging because serine levels can be influenced by multiple factors and exhibit variability between individuals. Therefore, early detection requires additional information such as family history or genotypic data (22,23). Understanding of the functions of PSAT1 is very important for understanding the cancer-promoting role of PSAT1 in tumors.

The present study demonstrated that overexpression of PSAT1 significantly potentiated proliferation, invasion and migration of ovarian cancer cells. Moreover, differential expression of PSAT1 was associated with the modulation of the malignant biological behavior. PSAT1 overexpression is a potential biomarker of favourable prognosis in patients with low-grade glioma (24). There is an association between increased PSAT1 expression and advanced clinical stage in patients with nasopharyngeal carcinoma (11). Furthermore, there is an association between PSAT1 expression levels and aggressive phenotypic characteristics in breast cancer, with higher expression being predictive of a poorer prognosis in primary cases, particularly in estrogen receptor-positive tumors (17,18). PSAT1 is upregulated in colorectal cancer tissue and associated with resistance to chemotherapy (25). The aforementioned findings are consistent with the present results, which indicated that PSAT1 promoted proliferation and invasion of cancer cells, suggesting that PSAT1 is a biomarker of poor prognosis in various malignancies, such as non-small cell lung cancer, oesophageal squamous cell carcinoma, breast and colorectal cancer (26,27).

Zheng *et al* (8) demonstrated that genes within a PSAT1 high expression mutant group were significantly enriched in a variety of pathways, including the 'cytokine-cytokine receptor interaction', 'Rap1 signalling pathway', 'chemokine signalling pathway', 'fox signalling pathway', 'TNF signalling pathway', 'mTOR signalling pathway' and other tumor-related signalling

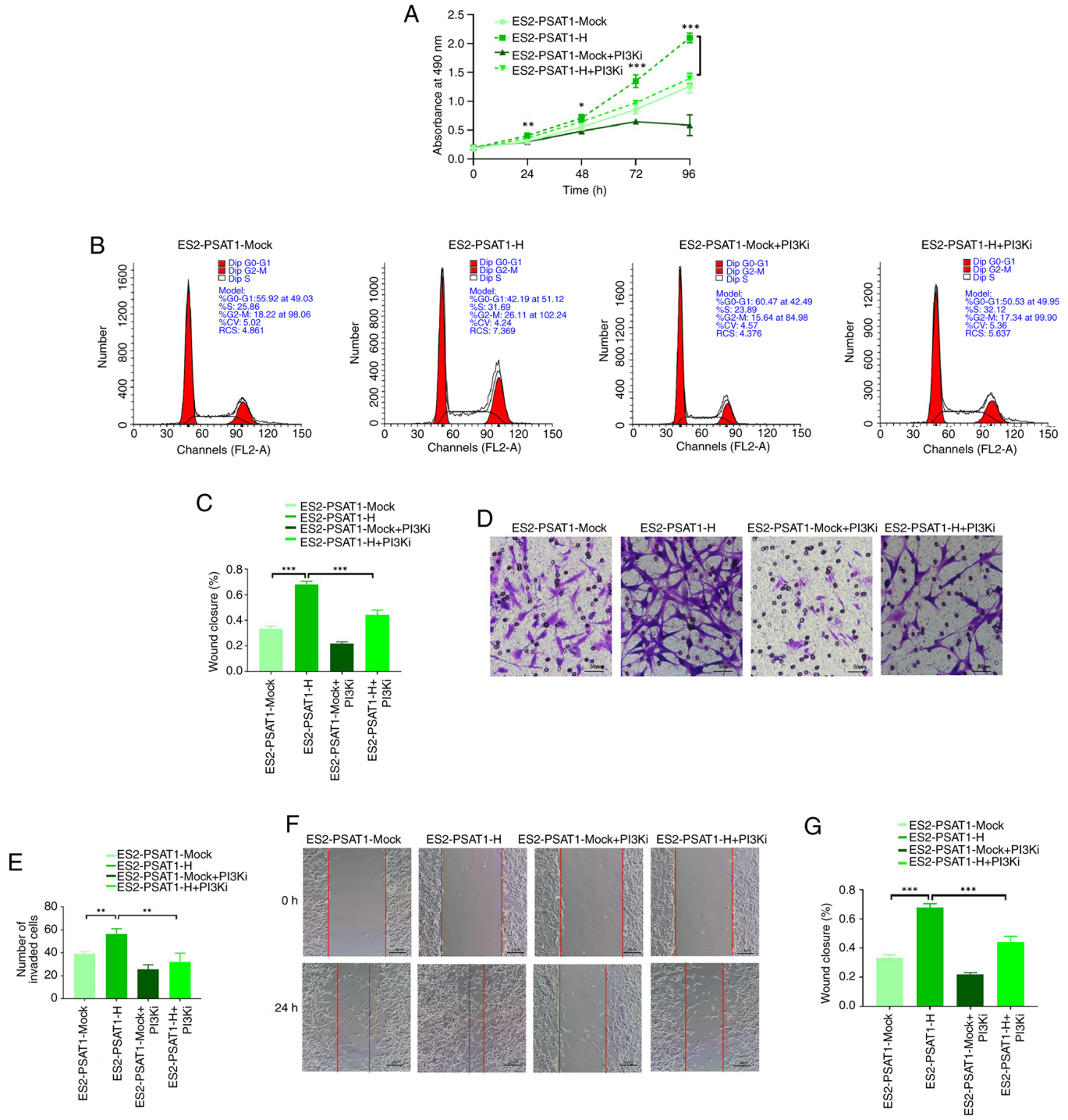


Figure 6. PI3Ki decreases proliferation, invasion, and migration abilities of ovarian cancer cells. (A) PI3Ki decreases proliferation (B) PI3Ki decreases the proportion of ovarian cells in S and G2/M phases. (C) Statistical analysis of cell cycle in ovarian cancer cells with PI3Ki. (D) PI3Ki decreased invasion ability. (E) Statistical analysis of cell invasion in ovarian cancer cells with PI3Ki. (F) PI3Ki decreased migration ability. (G) Statistical analysis of cell migration in ovarian cancer cells with PI3Ki. i, inhibitor; PSAT, phosphoserine aminotransferase; H, high. $^{*}$P<0.05; $^{**}$P<0.01; $^{***}$P<0.001 vs. control.

pathways. To the best of our knowledge, however, the aforementioned findings have not been experimentally corroborated in ovarian cancer tissue or cells. The levels of PSAT1 are increased in cisplatin-resistant cervical cancer cells (SiHa-R cells) (28). Knockdown of PSAT1 decreases the half-maximal inhibitory concentration of cisplatin, inhibits colony formation and promotes SiHa-R cell apoptosis (28). Suppression of PSAT1 expression inhibits proliferation and induces apoptosis by blocking the PI3K/AKT signalling pathway, thereby diminishing cisplatin resistance of SiHa-R cells. Consequently, PSAT1 is a potential therapeutic target for reversing cisplatin resistance in cervical cancer cells. In tumor cells, alterations in the serine-glycine amino acid biosynthetic pathway inhibit production of glutathione, thereby diminishing the capacity of cells to withstand oxidative stress and undergo programmed cell death (29,30). Conversely, upregulated expression of PSAT1 has been demonstrated to increase the ratio of reduced glutathione in ovarian cancer cells, conferring increased

resistance to oxidative damage and potentially facilitating aggressive progression of ovarian epithelial tumors (29,31-33).

PSAT1 exerts its functional effects by targeting proteins and transcription factors to modulate signaling pathways, such as the GSK3β/β-catenin and PI3K/AKT/mTOR pathways and influences biological processes by inhibiting autophagy mechanisms (34,35). Studies on intracranial aneurysms have demonstrated that the upregulation of microRNA (miR)-133a-3p and downregulation of PSAT1 ameliorate endothelial cell damage and enhance cell proliferation by suppressing the GSK3β/β-catenin pathway in intracranial aneurysms (34,35). Moreover, overexpression of miR-195-5p inactivates the GSK3β/β-catenin signalling pathway by suppressing PSAT1, thereby attenuating angiogenesis, decreasing chemoresistance to cisplatin and enhancing ovarian cancer cell apoptosis (36,37). PSAT1, which is upregulated in estrogen receptor-negative breast cancer, is activated by activating transcription factor 4 and promotes cell cycle progression by regulating the GSK3β/β-catenin/cyclin D1 pathway (36). miR-424, which is frequently downregulated in colorectal cancer, can inhibit the proliferation of colorectal cancer cells and induce apoptosis. Moreover, AKT3 and PSAT1 are direct targets of miR-424 (38). The loci of AKT3 and PSAT1 are implicated in miR-424 regulated apoptosis, underscoring the key role of miR-424 and its molecular targets, AKT3 and PSAT1, in the pathogenesis of colorectal cancer. Expression of PSAT1 in colorectal cancer is abnormally elevated due to G9A-mediated transcriptional activation, which not only activates the serine biosynthetic pathway but also provides α-ketoglutarate to facilitate entry into the tricarboxylic acid cycle. Downregulation of PSAT1 expression promotes cyclin D1 degradation through the mTOR pathway, culminating in cell cycle arrest and programmed cell death (39). These observations suggeste that PSAT1 represents a promising therapeutic target for colorectal cancer (39). In the present study, expression levels of PSAT1, p-PI3K and AKT were increased in ovarian cancer cells. Moreover, the invasive, migratory and proliferative capabilities of these cells were inhibited by PI3Ki, indicating that PSAT1 may bypass PI3K signaling and thereby impact the aggressive biological behaviors associated with ovarian cancer.

The STAT family comprises key cytokine-associated signalling mediators and potential molecular targets in cancer therapy that modulate invasion and metastasis. STAT4 expression is associated with prognosis of hepatocellular carcinoma (40). Furthermore, the identification of STAT4 as a regulator of KISS1 expression, which enhances the apoptosis of ovarian granulosa cells (41), underscoress its multifaceted role in cellular processes. Here, the suppression of STAT4 expression in ovarian cancer cells decreased PSAT1 protein levels, implicating STAT4 as a potential upstream transcriptional regulator of PSAT1.

A primary objective of translational research in precision medicine is to identify targeted therapeutics and predictive biomarkers, thereby facilitating the development of effective therapeutic strategies. Despite numerous inhibitors targeting the PI3K/AKT pathway currently undergoing preclinical trials (41,42), no PI3K or AKTi have received clinical approval to date. PI3K exists as a heterodimer composed of a catalytic and a regulatory subunit (43). Based on variations in catalytic subunits, PI3Ks can be classified into four isoforms: PI3Kα, PI3Kβ, PI3Kδ and PI3Kγ (4). Structural similarities between AKT isoforms and off-target inhibition within the cAMP-dependent protein kinase, cGMP-dependent protein kinase, and protein kinase C) kinase family pose challenges to achieving selectivity for AKTi (44). To date, no isomer of PSAT1 has been identified. The present findings indicated that targeting PSAT1 may offer therapeutic potential. If the high selectivity associated with PSAT1 can be effectively combined with potent inhibition of the PI3K/AKT pathway, this could yield improved clinical outcomes.

In conclusion, PSAT1 is a key player in serine metabolism that affects development and progression of tumors. The present study demonstrated elevated expression of PSAT1 in ovarian cancer through a combination of database and tissue-based experiments. By modulating activity of the PI3K/AKT signalling cascade, PSAT1 controls the proliferation, invasion and migration of ovarian cells, influencing malignant biological behaviors. The present results provide a theoretical foundation for PSAT1 as a prospective target for early detection and therapeutic management of ovarian cancer.

**Acknowledgements**

Not applicable.

**Funding**

The present study was supported by National Natural Science Foundation of China (grant nos. 82303503, 82203702 and 82173130), Key Research and Development Guidance Plan Project in Liaoning Province (grant no. 2019JH8/10300022) and Shenyang Science and Technology Program (grant nos. 22-315-6-16 and 22-321-33-19).

**Availability of data and materials**

The data generated in the present study may be requested from the corresponding author.

**Authors' contributions**

XL, SW and BL designed the study. YH and OL performed the experiments. XN and YW analyzed data. XL and SW edited the manuscript. XL and BL confirm the authenticity of all the raw data. All authors have read and approved the final manuscript.

**Ethics approval and consent to participate**

The present study was approved by Shengjing Hospital Affiliated to China Medical University Ethics Review Committee (approval no. 2021PS894K).

**Patient consent for publication**

Not applicable.

**Competing interests**

The authors declare that they have no competing interests.

## References


1. Arora T, Mullangi S, Vadakekut ES and Lekkala MR: Epithelial ovarian cancer. In: StatPearls. Treasure Island (FL): StatPearls Publishing, 2025.
2. Smith RA, Andrews KS, Brooks D, Fedewa SA, Manassaram-Baptiste D, Saslow D, Brawley OW and Wender RC: Cancer screening in the United States, 2018: A review of current American cancer society guidelines and current issues in cancer screening. CA Cancer J Clin 68: 297-316, 2018.
3. Zhang S, Xiao X, Yi Y, Wang X, Zhu L, Shen Y, Lin D and Wu C: Tumor initiation and early tumorigenesis: Molecular mechanisms and interventional targets. Signal Transduct Target Ther 9: 149, 2024.
4. Peng Y, Wang Y, Zhou C, Mei W and Zeng C: PI3K/Akt/mTOR pathway and its role in cancer therapeutics: Are we making headway? Front Oncol 12: 819128, 2022.
5. Mishra R, Patel H, Alanazi S, Kilroy MK and Garrett JT: PI3K inhibitors in cancer: Clinical implications and adverse effects. Int J Mol Sci 22: 3464, 2021.
6. Wang M, Zhang H, Lu Z, Su W, Tan Y, Wang J and Jia X: PSAT1 mediated EMT of colorectal cancer cells by regulating Pl3K/AKT signaling pathway. J Cancer 15: 3183-3198, 2024.
7. Zhang Y, Li J, Dong X, Meng D, Zhi X, Yuan L and Yao L: PSAT1 regulated oxidation-reduction balance affects the growth and prognosis of epithelial ovarian cancer. Onco Targets Ther 13: 5443-5453, 2020.
8. Zheng MJ, Li X, Hu YX, Dong H, Gou R, Nie X, Liu Q, Ying-Ying H, Liu JJ and Lin B: Identification of molecular marker associated with ovarian cancer prognosis using bioinformatics analysis and experiments. J Cell Physiol 234: 11023-11036, 2019.
9. Liu B, Jia Y, Cao Y, Wu S, Jiang H, Sun X, Ma J, Yin X, Mao A and Shang M: Overexpression of phosphoserine aminotransferase 1 (PSAT1) predicts poor prognosis and associates with tumor progression in human esophageal squamous cell carcinoma. Cell Physiol Biochem 39: 395-406, 2016.
10. Vié N, Copois V, Bascoul-Mollevi C, Denis V, Bec N, Robert B, Fraslon C, Conseiller E, Molina F, Larroque C, *et al*: Overexpression of phosphoserine aminotransferase PSAT1 stimulates cell growth and increases chemoresistance of colon cancer cells. Mol Cancer 7: 14, 2008.
11. Pollari S, Käkönen SM, Edgren H, Wolf M, Kohonen P, Sara H, Guise T, Nees M and Kallioniemi O: Enhanced serine production by bone metastatic breast cancer cells stimulates osteoclastogenesis. Breast Cancer Res Treat 125: 421-430, 2011.
12. Li H, Wu C, Chang W, Zhong L, Gao W, Zeng M, Wen Z, Mai S and Chen Y: Overexpression of PSAT1 is correlated with poor prognosis and immune infiltration in non-small cell lung cancer. Front Biosci (Landmark Ed) 28: 243, 2023.
13. Tang Z, Li C, Kang B, Gao G, Li C and Zhang Z: GEPIA: A web server for cancer and normal gene expression profiling and interactive analyses. Nucleic Acids Res 45 (W1): W98-W102, 2017.
14. Cancer Genome Atlas Research Network: Integrated genomic analyses of ovarian carcinoma. Nature 474: 609-615, 2011.
15. GTEx Consortium: Human genomics. The genotype-tissue expression (GTEx) pilot analysis: Multitissue gene regulation in humans. Science 348: 648-660, 2015.
16. Messeguer X, Escudero R, Farré D, Núñez O, Martínez J and Albà MM: PROMO: detection of known transcription regulatory elements using species-tailored searches. Bioinformatics 18: 333-334, 2002.
17. Sandelin A and Wasserman WW: Constrained binding site diversity within families of transcription factors enhances pattern discovery bioinformatics. J Mol Biol 338: 207-215, 2004.
18. Sirr A, Lo RS, Cromie GA, Scott AC, Ashmead J, Heyesus M and Dudley AM: A yeast-based complementation assay elucidates the functional impact of 200 missense variants in human PSAT1. J Inherit Metab Dis 43: 758-769, 2020.
19. van der Crabben SN, Verhoeven-Duif NM, Brilstra EH, Van Maldergem L, Coskun T, Rubio-Gozalbo E, Berger R and de Koning TJ: An update on serine deficiency disorders. J Inherit Metab Dis 36: 613-619, 2013.
20. Luo MY, Zhou Y, Gu WM, Wang C, Shen NX, Dong JK, Lei HM, Tang YB, Liang Q, Zou JH, *et al*: Metabolic and nonmetabolic functions of PSAT1 coordinate signaling cascades to confer EGFR inhibitor resistance and drive progression in lung adenocarcinoma. Cancer Res 82: 3516-3531, 2022.
21. Huang SP, Chan YC, Huang SY and Lin YF: Overexpression of PSAT1 gene is a favorable prognostic marker in lower-grade gliomas and predicts a favorable outcome in patients with IDH1 mutations and chromosome 1p19q Codeletion. Cancers (Basel) 12: 13, 2019.
22. Acuna-Hidalgo R, Schanze D, Kariminejad A, Nordgren A, Kariminejad MH, Conner P, Grigelioniene G, Nilsson D, Nordenskjöld M, Wedell A, *et al*: Neu-Laxova syndrome is a heterogeneous metabolic disorder caused by defects in enzymes of the L-serine biosynthesis pathway. Am J Hum Genet 95: 285-293, 2014.
23. Moat S, Carling R, Nix A, Henderson M, Briddon A, Prunty H, Talbot R, Powell A, Wright K, Fuchs S and de Koning T: Multicentre age-related reference intervals for cerebrospinal fluid serine concentrations: Implications for the diagnosis and follow-up of serine biosynthesis disorders. Mol Genet Metab 101: 149-152, 2010.
24. Liao KM, Chao TB, Tian YF, Lin CY, Lee SW, Chuang HY, Chan TC, Chen TJ, Hsing CH, Sheu MJ and Li CF: Overexpression of the PSAT1 gene in nasopharyngeal carcinoma is an indicator of poor prognosis. J Cancer 7: 1088-1094, 2016.
25. De Marchi T, Timmermans MA, Sieuwerts AM, Smid M, Look MP, Grebenchtchikov N, Sweep FCGJ, Smits JG, Magdolen V, van Deurzen CHM, *et al*: Phosphoserine aminotransferase 1 is associated to poor outcome on tamoxifen therapy in recurrent breast cancer. Sci Rep 7: 2099, 2017.
26. Qian C, Xia Y, Ren Y, Yin Y and Deng A: Identification and validation of PSAT1 as a potential prognostic factor for predicting clinical outcomes in patients with colorectal carcinoma. Oncol Lett 14: 8014-8020, 2017.
27. Jia L, Li D, Wang YN, Zhang D and Xu X: PSAT1 positively regulates the osteogenic lineage differentiation of periodontal ligament stem cells through the ATF4/PSAT1/Akt/GSK3β/β-catenin axis. J Transl Med 21: 70, 2023.
28. Fang Y, Liang X, Xu J and Cai X: miR-424 targets AKT3 and PSAT1 and has a tumor-suppressive role in human colorectal cancer. Cancer Manag Res 10: 6537-6547, 2018.
29. Duan W and Liu X: PSAT1 upregulation contributes to cell growth and cisplatin resistance in cervical cancer cells via regulating PI3K/AKT signaling pathway. Ann Clin Lab Sci 50: 512-518, 2020.
30. Hui Z, Wang X and Li X: Targeting the serine-glycine one-carbon pathway overcomes glutathione-mediated drug resistance in cancer. Cell Death Dis 10: 52, 2019.
31. Moloney JN and Cotter TG: ROS signalling in the biology of cancer. Semin Cell Dev Biol 80: 50-64, 2018.
32. Smith CL, Bolton A and Nguyen G: Genomic and epigenomic instability, fragile sites, schizophrenia and autism. Curr Genomics 11: 447-469, 2010.
33. Butturini E, Carcereri de Prati A, Boriero D and Mariotto S: Natural sesquiterpene lactones enhance chemosensitivity of tumor cells through redox regulation of STAT3 signaling. Oxid Med Cell Longev 2019: 4568964, 2019.
34. Lv H, Zhen C, Liu J, Yang P, Hu L and Shang P: Unraveling the potential role of glutathione in multiple forms of cell death in cancer therapy. Oxid Med Cell Longev 2019: 3150145, 2019.
35. Gao S, Ge A, Xu S, You Z, Ning S, Zhao Y and Pang D: PSAT1 is regulated by ATF4 and enhances cell proliferation via the GSK3β/β-catenin/cyclin D1 signaling pathway in ER-negative breast cancer. J Exp Clin Cancer Res 36: 179, 2017.
36. Jia Q, Yan S, Huang J and Xu S: Restored microRNA-133a-3p or depleted PSAT1 restrains endothelial cell damage-induced intracranial aneurysm via suppressing the GSK3β/β-catenin pathway. Nanoscale Res Lett 15: 177, 2020.
37. Wang H, Fang Q, You S, Wu Y and Zhang C: miRNA-195-5p/PSAT1 feedback loop in human triple-negative breast cancer cells. Genes Genomics 45: 39-47, 2023.
38. Wang H, Cui L, Li D, Fan M, Liu Z, Liu C, Pan S, Zhang L, Zhang H and Zhao Y: Overexpression of PSAT1 regulated by G9A sustains cell proliferation in colorectal cancer. Signal Transduct Target Ther 5: 47, 2020.
39. Wang G, Chen JH, Qiang Y, Wang DZ and Chen Z: Decreased STAT4 indicates poor prognosis and enhanced cell proliferation in hepatocellular carcinoma. World J Gastroenterol 21: 3983-3993, 2015.
40. Jiang Y, Xin X, Pan X, Zhang A, Zhang Z, Li J and Yuan X: STAT4 targets KISS1 to promote the apoptosis of ovarian granulosa cells. J Ovarian Res 13: 135, 2020.

41. Yu L, Wei J and Liu P: Attacking the PI3K/Akt/mTOR signaling pathway for targeted therapeutic treatment in human cancer. Semin Cancer Biol 85: 69-94, 2022.
42. Ediriweera MK, Tennekoon KH and Samarakoon SR: Role of the PI3K/AKT/mTOR signaling pathway in ovarian cancer: Biological and therapeutic significance. Semin Cancer Biol 59: 147-160, 2019.
43. Wymann MP and Pirola L: Structure and function of phosphoinositide 3-kinases. Biochim Biophys Acta 1436: 127-150, 1998.
44. Quambusch L, Depta L, Landel I, Lubeck M, Kirschner T, Nabert J, Uhlenbrock N, Weisner J, Kostka M and Levy LM,: Cellular model system to dissect the isoform-selectivity of Akt inhibitors. Nat Commun 12: 5297, 2021.